Biochemical and Biophysical Research Communications 435 (2013) 334–338

Contents lists available at SciVerse ScienceDirect

Biochemical and Biophysical Research Communications

journal homepage: www.elsevier.com/locate/ybbrc

Crystal structure of the guanylate kinase domain from discs large homolog 1 (DLG1/SAP97)

Shinji Mori [a,b], Yuta Tezuka [a,c], Akihiko Arakawa [a,b], Noriko Handa [b], Mikako Shirouzu [b], Tetsu Akiyama [c], Shigeyuki Yokoyama [a,b,*]

[a] Department of Biophysics and Biochemistry, Graduate School of Science, The University of Tokyo, Bunkyo-ku, Tokyo 113-0033, Japan
[b] RIKEN Systems and Structural Biology Center, Tsurumi-ku, Yokohama 230-0045, Japan
[c] Institute Molecular and Cellular Biosciences, The University of Tokyo, Bunkyo-ku, Tokyo 113-0032, Japan

ARTICLE INFO

Article history:
Received 12 April 2013
Available online 25 April 2013

Keywords:
X-ray crystallography
MAGUK family
GK domain
Peptide binding
Scaffold

ABSTRACT

Discs large homolog 1 (DLG1/SAP97) is involved in the development and regulation of neuronal and immunological synapses. DLG1 is a member of the membrane associated guanylate kinase (MAGUK) family of proteins, which function as molecular scaffolds. The C-terminal guanylate kinase (GK) domain of DLG1 binds peptides with a phosphorylated serine residue. In this study, we solved the crystal structure of the GK domain of human DLG1. The C-terminal tail of DLG1 is bound to the peptide-binding site of an adjacent symmetry-related DLG1 GK molecule. The binding direction of the C-terminal tail to the peptide-binding site is opposite to that of the phosphorylated LGN peptide in complex with the rat DLG1 GK domain. The C-terminal tail forms a 3_{10} helix, which is also different from the conformation of the phosphorylated LGN peptide. Nevertheless, the side chain interactions of the C-terminal tail with the DLG1 GK domain are similar to those of the phosphorylated LGN peptide.

1. Introduction

The discs large (DLG) tumor suppressor from *Drosophila* and its mammalian homologue DLG1, also known as synapse-associated protein 97 (SAP97), belong to the membrane-associated guanylate kinase (MAGUK) family of proteins, which function as molecular scaffolds for the assembly of protein complexes at cell–cell contact sites [1–5]. The MAGUK proteins consist of three conserved domains: one or more PDZ domains, a Src-homology 3 (SH3) domain, and a guanylate kinase (GK) domain. The GK domains of the MAGUK family proteins are catalytically inactive [6,7], and instead are involved in protein–protein interactions.

DLG1 is expressed in neuronal cells, lymphocytes, and epithelial cells. In neuronal synapses, DLG1 binds to glutamate receptor subtypes, and transports them to the plasma membrane [2,3]. In T lymphocytes, DLG1 is translocated to immunological synapses in response to T cell receptor (TCR) engagement, and mediates TCR-induced signaling [4]. DLG1 knockout mice exhibit developmental abnormalities in their renal and urogenital organs [5]. The DLG1 GK domain binds to several proteins, such as guanylate kinase-associated protein (GKAP)/discs large-associated protein 1 (DLGAP1)/SAP90/PSD-95-associated protein 1 (SAPAP1) [8], microtubule-associated protein 1A (MAPlA) [9], guanylate kinase associated kinesin (GAKIN)/kinesin superfamily protein 13B (KIF13B) [10], brain-enriched guanylate kinase-associated protein (BEGAIN) [11], SPA-1-like protein (SPAL)/spine-associated RAP-specific GTPase activating protein (SPAR) [12], and leucine–glycine–asparagine repeat protein (LGN) [13,14].

A recent report found that the SH3-GK fragment of rat DLG1 binds various phosphorylated peptides [13]. The crystal structure of the fragment in complex with the phosphorylated LGN (p-LGN) peptide revealed that it is bound in a site corresponding to the guanosine monophosphate (GMP)-binding site of the catalytically active GK enzymes [13]. Thus, the consensus motif for phosphorylation-dependent binding to the GK domain was proposed [13].

In the present study, we solved the crystal structure of the GK-domain fragment of human DLG1. In the crystal, the C-terminal tail of one DLG1 molecule is bound to the phosphorylated peptide-binding site of a symmetry-related DLG1 molecule. The conformation and the direction of the C-terminal tail are both completely different from those of the p-LGN peptide in the DLG1 complex, while the side-chain interactions of Glu924 in the C-terminal tail with the DLG1 GK domain are similar to those of the phosphoserine (pSer) residue of the p-LGN peptide.

* Corresponding author. Address: RIKEN Systems and Structural Biology Center, 1-7-22 Suehiro-cho, Tsurumi-ku, Yokohama 230-0045, Japan. Fax: +81 45 503 9195.
E-mail address: yokoyama@riken.jp (S. Yokoyama).

0006-291X
http://dx.doi.org/10.1016/j.bbrc.2013.04.056

2. Materials and methods

2.1. Protein expression and purification

The GK domain of human DLG1 (amino acid residues 734–926: the residue numbers are of the 926-residue splice variant), with an N-terminal histidine-affinity tag and a tobacco etch virus (TEV) protease cleavage site, was cloned into the pCR2.1-TOPO vector (Invitrogen). The selenomethionine-substituted protein was expressed using the *Escherichia coli* cell-free system. The protein was purified by chromatography on a HisTrap column (GE Healthcare Bio-Sciences), and was subjected to TEV protease digestion. The cleaved histidine-affinity tag was removed by a second passage through the HisTrap column. The flowthrough fraction was collected and loaded on a HiTrap Q column (GE Healthcare Bio-Sciences) and a Superdex 200 column (GE Healthcare Bio-Sciences). The protein sample was concentrated to 6.5 mg ml^{-1} in 20 mM Tris–HCl buffer (pH 8.0), containing 150 mM NaCl and 2 mM dithiothreitol (DTT).

2.2. Crystallization, data collection, and structure determination

The crystal was obtained by the hanging-drop vapor-diffusion method at 20 °C, with a reservoir solution containing 0.2 M sodium thiocyanate and 22% polyethylene glycol (PEG) 3350. The diffraction data were collected at the BL26B2 beamline of SPring-8 (Harima, Japan), and were processed with HKL2000 [15]. The crystal belongs to the space group $P6_522$, with one molecule in the crystallographic asymmetry unit. The structure was determined by a combination of molecular replacement and selenomethionine single-wavelength anomalous dispersion (SAD), using the PSD-95 GK domain (Protein Data Bank (PDB) code 1JXO) as a search model, by Phenix [16]. Model building was accomplished with Coot [17], and refinement was performed with CNS [18] and Phenix [16]. Data collection and refinement statistics are summarized in Table 1. The final models had no Ramachandran violations, as confirmed by PROCHECK [19]. The figures were generated by Pymol (http://pymol.sourceforge.net/).

Table 1
Data collection, phasing, and refinement statistics.

Data collection	
Beamline	SPring-8 BL26B2
Space group	$P6_522$
Unit cell	
a, *b*, *c* (Å)	65.535, 65.535, 180.563
α, β, γ (°)	90.0, 90.0, 120.0
Wavelength (Å)	0.979077
Resolution (Å)	50–2.20 (2.28–2.20)*
Completeness (%)	98.2 (97.6)
Redundancy	12.0 (6.4)
$I/\sigma(I)$	25.3 (2.9)
*R*sym†	0.077 (0.409)
No. monomers/asymmetric unit	1
Refinement	
Resolution (Å)	48.0–2.20
No. reflections	21,563
*R*work/*R*free§	0.209/0.265
No. protein atoms	1434
No. water molecules	61
RMSD bond lengths (Å)	0.008
RMSD bond angles (°)	1.001
Ramachandran plot	
Most favored regions (%)	91.6
Additional allowed regions (%)	8.4

* The statistics in the highest-resolution shell are given in parentheses.
† *R*sym = $\sum|I - \langle I\rangle|/\sum I$, where *I* is the observed intensity of reflections.
§ *R*work, free = $\sum|Fobs - Fcalc|/\sum Fobs$. Free reflections consist of 10% of the total number of reflections.

2.3. PDB accession numbers

The atomic coordinates and structure factors have been deposited in the PDB, with the accession code 3W9Y.

3. Results and discussion

3.1. Overall structure of the DLG1 GK domain

The crystal structure of the GK domain of human DLG1 (734–926) was solved at 2.2 Å resolution. The crystal belongs to the space group $P6_522$, with one molecule in the asymmetric unit. The topology is similar to those of the published GK-domain structures of other proteins (Fig. 1B). The present structure contains six α helices, α1–α5 and α7, and nine β strands, β1–β9 (Fig. 1B). The CORE subdomain of the GK domain is composed of α1, α3, α4, α7, β1, β2, and β7–β9, and the nucleoside monophosphate (NMP)-binding subdomain contains α2 and β3–β6 (Fig. 1B). Residues 858–875 are missing in the present electron-density map (Fig. 1B), presumably due to disorder, while in the DLG1 GK-domain structures, these residues belong to the LID subdomain, which consists of the α5 and α6 helices and the loop between them [13,20]. The N-terminal artificial linker of the present construct is also disordered in the crystal.

The DLG1 GK structure adopts an open conformation, which corresponds to those of the DLG1 GK domain complexed with the p-LGN peptide [13], the GK domain of PSD-95 [21,22], and

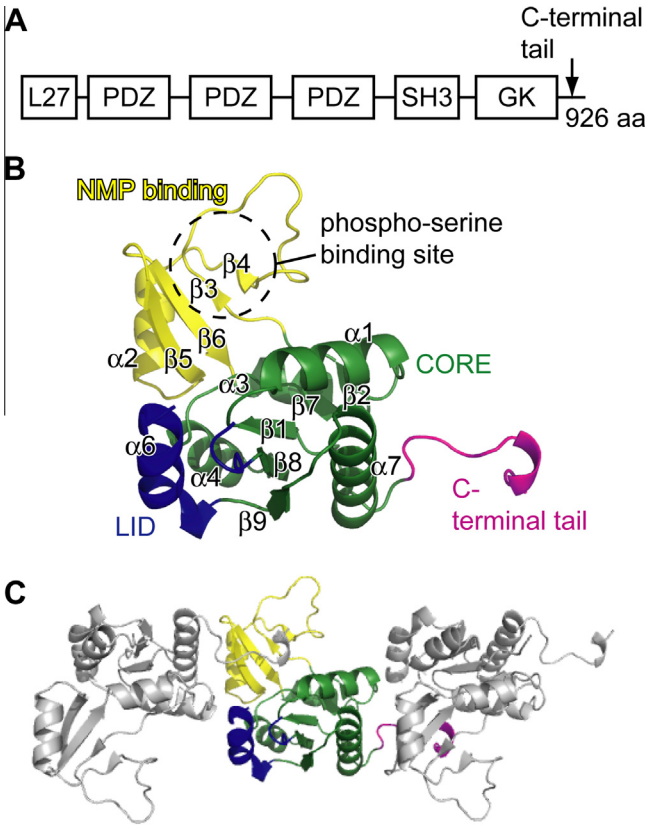

Fig. 1. The crystal structure of the GK domain of human DLG1. (A) The domain composition of DLG1. (B) The crystal structure of the DLG1 GK domain. The CORE subdomain (green), the nucleoside monophosphate-binding subdomain (yellow), the LID subdomain (blue), and the C-terminal tail (magenta) are indicated in the ribbon model. (C) Interactions between the symmetry-related molecules. The central molecule is colored as in (B), and the adjacent molecules are colored grey.

the homologous GK enzyme from yeast without GMP [23] (Fig. 2). On the other hand, the yeast GK enzyme assumes a closed conformation in the GMP-bound state [23] (Fig. 2C). Unlike the yeast GK enzyme, the GK domains of DLG1 and PSD-95 do not exhibit the kinase activity [6,7]. The GK domains of the MAGUK family proteins are thought to lack the dynamic structural change between the open and closed conformations, and thereby assume only the constitutively open conformation [24].

3.2. The peptide-binding site and the C-terminal tail of the DLG1 GK domain

In the DLG1 GK structure, the NMP-binding subdomain of one molecule is bound to the C-terminal tail of an adjacent symmetry-related molecule, while its own tail is bound to the NMP-binding subdomain of another symmetry-related molecule (Fig. 1C). Due to these consecutive interactions in the crystal, the GK-domain molecules form multimers with an approximately linear arrangement. The NMP-binding subdomain contains a cluster of positively charged residues, and provides the binding site for the phosphorylated peptide [13]. It is remarkable that this intermolecular interaction occurs without the phosphorylation of the C-terminal tail.

The interaction between the phosphorylated peptide-binding site and the C-terminal tail is too weak to form multimers in solution. A size exclusion chromatography analysis indicated that the GK domain is monomeric at 0.8 mg ml^{-1} in solution (data not shown).

The C-terminal tail forms a short 3_{10} helix, from Pro921 to Lys925 (Figs. 1B and 3A). In contrast, the C-terminal tail (Tyr902–Pro906, corresponding to Tyr917–Pro921 in human DLG1) of the rat DLG1 SH3–GK domain forms a β strand that interacts with the fifth β strand in the SH3 domain, as an anti-parallel β sheet [13]. Various structures containing both the SH3 and GK domains of typical MAGUK family proteins have been solved [13,20–22,25–27]. The structures revealed that all of the C-terminal tails form antiparallel β sheets with the fifth β strands of the SH3 domains [13,20–22,25–27]. The C-terminal tail is required for the regulation of MAGUK function [28,29]. Models built based on the crystal structures and biochemical assays suggested that MAGUK oligomerization occurs through the exchange of the fifth β strand of the SH3 domain [21]. On the other hand, the expression construct of DLG1 used in the present study lacks the SH3 domain, while it retains the C-terminal tail.

3.3. Mechanisms of the interaction of the peptide-binding site with the C-terminal tail

The DLG1 C-terminal tail, which is well defined in the electron density map, interacts with the phosphorylated peptide-binding site (Fig. 3A). The C-terminal 10 residues, from Tyr917 to Leu926, are extended to the adjacent GK domain in the crystal, and interact mainly with the NMP-binding subdomain, which includes the peptide-binding site (Fig. 3A).

The hydroxyl group of Tyr917 forms a direct hydrogen bond with the side chain of Asn807 and a water-mediated hydrogen bond with the hydroxyl group of Tyr806 (Fig. 3A). The main-chain amide and carbonyl groups of Trp919 form water-mediated hydrogen bonds with the main-chain carbonyl of Gln805 (Fig. 3A). The side chain of Trp919 hydrogen bonds with the side chain of Glu802, and forms a hydrophobic contact with the ring of Pro921 (Fig. 3A). In turn, the Pro921 ring forms hydrophobic contacts with the aromatic rings of Tyr806 and Tyr811. The side chain of Lys923 hydrogen bonds with the main-chain carbonyl group of Asp781 (Fig. 3A). The side chain of Glu924 forms direct hydrogen bonds with the side chains of Arg770, Tyr782, and Tyr811, and water-mediated hydrogen bonds with the side chains of Arg773 and Tyr806 (Fig. 3A). The main chain of Glu924 also forms a water-mediated hydrogen bond with the hydroxyl group of Tyr806. The side chain of Lys925 hydrogen bonds with the side chain of Asp831 (Fig. 3A).

3.4. Comparison of the C-terminal tail with the p-LGN peptide complexed with DLG1

The structural comparison revealed some dramatic differences. First of all, the main-chain direction of the C-terminal tail of DLG1 is opposite to that of the p-LGN peptide (Fig. 3A and B) [13]. In addition, the peptide conformations are also different from each other. The residues from Pro921 to Lys925 in the C-terminal tail form a short 3_{10} helix in the present structure, while the p-LGN peptide in the previous DLG1 complex structure includes an α helix [from His(−1) to Glu(+2)] and a β strand [Glu(+5) and Leu(+6)] (numbering from the pSer residue at position 0 [pSer(0)], which corresponds to Ser401 in rat LGN) (Fig. 3A and B) [13]. A structural superposition revealed that the α helix axis in the p-LGN peptide is almost perpendicular to the 3_{10} helix axis in the C-terminal tail (Fig. 3A and B) [13].

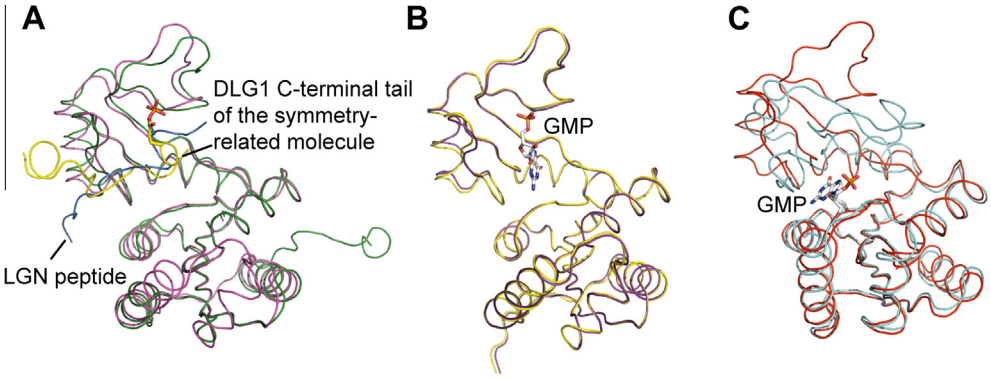

Fig. 2. Structural comparisons of the MAGUK GK domains and the GK enzyme. (A) The human DLG1 GK domain with the C-terminal tail (PDB ID: 3W9Y) and the rat DLG1 GK domain complexed with the p-LGN peptide (PDB ID: 3UAT). The human DLG1 GK domain is shown with the C-terminal tail depicted as a green tube model, the C-terminal tail of the symmetry-related molecule shown as a yellow tube model, and Glu924 represented by a yellow stick model. The rat DLG1 GK domain and the p-LGN peptide are represented by magenta and blue tube models, respectively, with pSer(0) of the p-LGN peptide depicted by a blue stick model. (B) The rat PSD-95 GK domain in the apo-form (yellow) (PDB ID: 1KJW) and in the GMP-bound form (purple) (PDB ID: 1JXM). The GMP molecule is represented by a white stick model. (C) The yeast GK enzyme in the apo-form (red) (PDB ID: 1EX6) and in the GMP-bound form (cyan) (PDB ID: 1EX7). The GMP molecule is represented by a white stick model.

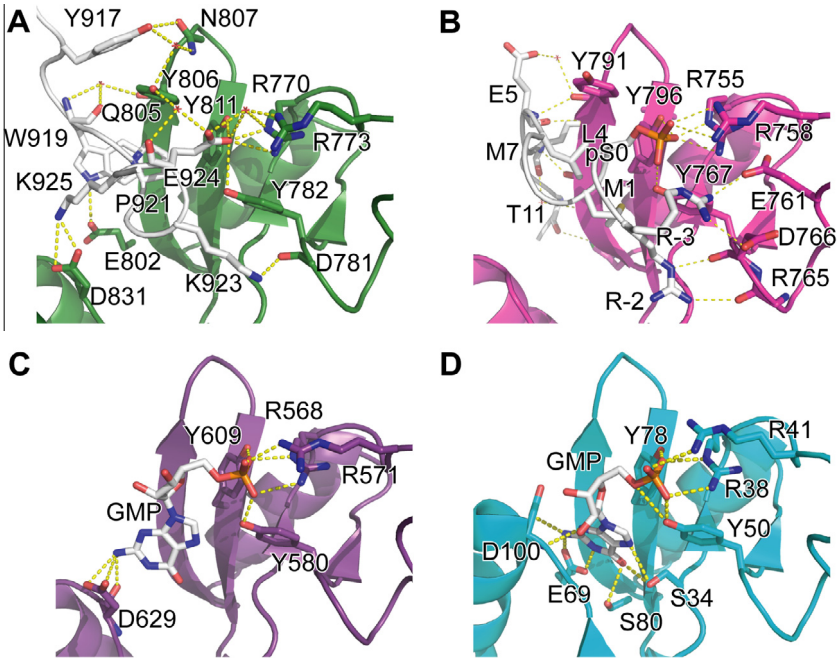

Fig. 3. Ligand-binding interfaces of the MAGUK GK domain and the GK enzyme. (A) The present human DLG1 GK domain (PDB ID: 3W9Y). The human DLG1 GK domain with the C-terminal tail is represented by a green ribbon model, while the C-terminal tail of the symmetry-related molecule is represented by a white tube model. (B) The rat DLG1 GK domain (PDB ID: 3UAT). The rat DLG1 GK domain and the p-LGN peptide are represented by the magenta ribbon model and the white tube model, respectively. (C) The rat PSD-95 GK domain (purple ribbon model) and GMP (white stick model) (PDB ID: 1JXM). (D) The yeast GK enzyme (cyan ribbon model) and GMP (white stick model) (PDB ID: 1EX7). Hydrogen bonds are indicated with yellow dashed lines.

The reason why the GK domain can bind the two peptides in opposite directions is because the side chains of these peptides bind in similar manners to the GK domain. First, Glu924, which mimics the charge of the pSer residue, is in a similar position to that occupied by pSer(0) of the p-LGN peptide [13] (Fig. 3A and B). Glu924 forms direct hydrogen bonds with the side chains of Arg770, Tyr782, and Tyr811, as well as a water-mediated hydrogen bond with Arg773 (Fig. 3A). In the rat DLG1·p-LGN peptide complex, pSer(0) of the p-LGN peptide forms direct hydrogen bonds with the side chains of Arg755, Arg758, Tyr767, and Tyr796, corresponding to Arg770, Arg773, Tyr782, and Tyr811 of human DLG1 [13] (Fig. 3B). Since the distance between the side chains of Glu924 and Arg773 in human DLG1 is much longer than that between the pSer(0) and Arg758 in the rat DLG1·p-LGN peptide complex, the stable water that mediates the hydrogen bonding interaction between the side chains of Glu924 and Arg773 in human DLG1 may be important for reinforcing the complex. Second, Trp919 and Pro921 occupy similar positions to those of Met(+1) and Leu(+4), respectively, of the p-LGN peptide complex [13] (Fig. 3A and B). The side chains of Trp919 and Pro921 form hydrophobic interactions in similar manners to Met(+1) and Leu(+4) in the p-LGN complex (Fig. 3A and B). Third, Lys923 occupies a comparable position to Arg(−2) in the p-LGN complex [13] (Fig. 3A and B). Lys923 and Arg(−2) form hydrogen bonds with the main-chain carbonyl group of Asp (Asp781 and Asp766, respectively) in the pSer-binding loop (Fig. 3A and B).

In addition to the side chains, the main chain of the DLG1 C-terminal tail forms three water-mediated hydrogen bonds with the binding site (the main-chain carbonyl group of Glu924 and the side chain of Tyr806; the main-chain amide group of Trp919 and the main-chain carbonyl group of Gln805; and the main-chain carbonyl group of Trp919 and the main-chain carbonyl group of Gln805) (Fig. 3A). In contrast, the main chain of the p-LGN peptide forms four direct hydrogen bonds (the main-chain carbonyl group of Glu(+5) and the main-chain amide of Gln790, the main-chain amide group of Glu(+5) and the main-chain carbonyl group of Gln790, the main-chain amide group of Met(+7) and the main-chain carbonyl group of Ala788, and the main-chain carbonyl group of Thr(+11) and the side chain of His783) and one water-mediated hydrogen bond (the main-chain carbonyl group of Met(+7) and the main-chain amide group of Ala788) with DLG1 [13] (Fig. 3B). The lack of direct hydrogen bonds between the main chain of the DLG1 C-terminal tail and DLG1 allows the C-terminal tail to be bound in the opposite direction to the p-LGN peptide.

The side chains of Asp629 in human PSD-95 and Glu69 in the yeast GK enzyme form hydrogen bonds with the 2-amino group of GMP in the GMP complex structures (Fig. 3C and D) [22,23]. The corresponding residues of human DLG1 are Asp831 and Glu802, respectively, and their side chains hydrogen bond with those of Tyr919 and Lys925, respectively, in the C-terminal tail (Fig. 3A, C and D). These interactions are not seen in the p-LGN peptide complex. Hence, these additional interactions seem to be necessary to bind the C-terminal tail peptide in the direction opposite to that of the p-LGN peptide.

The present structure may mimic the state in which the C-terminal tail of the GK domain dissociates from the fifth β strand of the SH3 domain. The Wiskott–Aldrich syndrome protein (WASP), or presumably its polyproline sequence, binds to the SH3 domain [30]. Calmodulin and protein 4.1 also bind to the HOOK region, which is inserted between the fourth and fifth β strands of the SH3 domain [31,32]. These proteins may prevent the C-terminal tail from interacting with the SH3 domain, and induce the binding of the C-terminal tail to the pSer-binding site. Similar amino-acid sequences to that of the DLG1 C-terminal tail may have the potential to interact with the phosphorylated peptide-binding site. Our structure provides information about possible DLG1-binding motifs and their binding modes.

Acknowledgments

The authors are grateful to Dr. T. Terada for advice on protein purification and to Dr. H. Niwa and the beamline staff at SPring-8 BL26B2 (Hyogo, Japan) for support with X-ray data collection. This work was supported by the RIKEN Structural Genomics/Proteomics Initiative (RSGI), the National Project on Protein Structural and Functional Analyses, and the Targeted Proteins Research Program from the Ministry of Education, Culture, Sports, Science, and Technology of Japan.

References

[1] L. Funke, S. Dakoji, D.S. Bredt, Membrane-associated guanylate kinases regulate adhesion and plasticity at cell junctions, Annu. Rev. Biochem. 74 (2005) 219–245, http://dx.doi.org/10.1146/annurev.biochem.74.082803.133339. <http://www.annualreviews.org/doi/full/10.1146/annurev.biochem.74.082803.133339> (accessed 1.03.2013).

[2] D. Mauceri, F. Gardoni, E. Marcello, M. Di Luca, Dual role of CaMKII-dependent SAP97 phosphorylation in mediating trafficking and insertion of NMDA receptor subunit NR2A, J. Neurochem. 100 (2007) 1032–1046, http://dx.doi.org/10.1111/j.1471-4159.2006.04267.x. <http://onlinelibrary.wiley.com/doi/10.1111/j.1471-4159.2006.04267.x/full> (accessed 1.03.2013).

[3] N. Sans, C. Racca, R.S. Petralia, et al., Synapse-associated protein 97 selectively associates with a subset of AMPA receptors early in their biosynthetic pathway, J. Neurosci. 21 (2001) 7506–7516. <http://www.jneurosci.org/content/21/19/7506.abstract> (accessed 1.03.2013).

[4] J.L. Round, T. Tomassian, M. Zhang, et al., Dlgh1 coordinates actin polymerization, synaptic T cell receptor and lipid raft aggregation, and effector function in T cells, J. Exp. Med. 201 (2005) 419–430, http://dx.doi.org/10.1084/jem.20041428. <http://jem.rupress.org/content/201/3/419.abstract> (accessed 1.03.2013).

[5] A. Iizuka-Kogo, T. Ishidao, T. Akiyama, T. Senda, Abnormal development of urogenital organs in Dlgh1-deficient mice, Development 134 (2007) 1799–1807, http://dx.doi.org/10.1242/dev.02830. <http://dev.biologists.org/content/134/9/1799.short> (accessed 1.03.2013).

[6] S. Kuhlendahl, O. Spangenberg, M. Konrad, et al., Functional analysis of the guanylate kinase-like domain in the synapse-associated protein SAP97, Eur. J. Biochem. 252 (1998) 305–313, http://dx.doi.org/10.1046/j.1432-1327.1998.2520305.x. <http://onlinelibrary.wiley.com/doi/10.1046/j.1432-1327.1998.2520305.x/abstract> (accessed 1.03.2013).

[7] O. Olsen, D.S. Bredt, Functional analysis of the nucleotide binding domain of membrane-associated guanylate kinases, J. Biol. Chem. 278 (2003) 6873–6878, http://dx.doi.org/10.1074/jbc.M210165200. <http://www.jbc.org/content/278/9/6873.short> (accessed 1.03.2013).

[8] E. Kim, S. Naisbitt, Y.P. Hsueh, et al., GKAP, a novel synaptic protein that interacts with the guanylate kinase-like domain of the PSD-95/SAP90 family of channel clustering molecules, J. Cell Biol. 136 (1997) 669–678, http://dx.doi.org/10.1083/jcb.136.3.669. <http://jcb.rupress.org/content/136/3/669.abstract> (accessed 1.03.2013).

[9] J.E. Brenman, J.R. Topinka, E.C. Cooper, et al., Localization of postsynaptic density-93 to dendritic microtubules and interaction with microtubule-associated protein 1A, J. Neurosci. 18 (1998) 8805–8813. <http://www.jneurosci.org/content/18/21/8805.abstract> (accessed March 1, 2013).

[10] T. Hanada, L. Lin, E.V. Tibaldi, et al., GAKIN, a novel kinesin-like protein associates with the human homologue of the *Drosophila* discs large tumor suppressor in T lymphocytes, J. Biol. Chem. 275 (2000) 28774–28784, http://dx.doi.org/10.1074/jbc.M000715200. <http://www.jbc.org/content/275/37/28774.short>(accessed 1.03.2013).

[11] M. Deguchi, Y. Hata, M. Takeuchi, et al., BEGAIN (brain-enriched guanylate kinase-associated protein), a novel neuronal PSD-95/SAP90-binding protein, J. Biol. Chem. 273 (1998) 26269–26272, http://dx.doi.org/10.1074/jbc.273.41.26269. <http://www.jbc.org/content/273/41/ 26269.short> (accessed1.03 2013).

[12] D.T.S. Pak, S. Yang, S. Rudolph-Correia, et al., Regulation of dendritic spine morphology by SPAR, a PSD-95-associated RapGAP, Neuron 31 (2001) 289–303, http://dx.doi.org/10.1016/S0896-6273(01)00355-5. <http://www.sciencedirect.com/science/article/pii/S0896627301003555> (accessed 1.03.2013).

[13] J. Zhu, Y. Shang, C. Xia, et al., Guanylate kinase domains of the MAGUK family scaffold proteins as specific phospho-protein-binding modules, EMBO J. 30 (2011) 4986–4997, http://dx.doi.org/10.1038/emboj.2011.428. <http://www.nature.com/emboj/journal/v30/n24/abs/emboj2011428a.html> (accessed 1.03.2013).

[14] N. Sans, P.Y. Wang, Q. Du, et al., MPins modulates PSD-95 and SAP102 trafficking and influences NMDA receptor surface expression, Nat. Cell Biol. 7 (2005) 1179–1190, http://dx.doi.org/10.1038/ncb1325. <http://www.nature.com/ncb/journal/v7/n12/abs/ncb1325.html> (accessed 1.03. 2013).

[15] Z. Otwinowski, W. Minor, Processing of X-ray diffraction data collected in oscillation mode, Meth. Enzymol. 276 (1997) 307–326, http://dx.doi.org/10.1016/S0076-6879(97)76066-X. <http://www.sciencedirect.com/science/article/pii/S007668799776066X> (accessed 1.03.2013).

[16] P.D. Adams, P.V. Afonine, G. Bunkoczi, et al., PHENIX: a comprehensive python-based system for macromolecular structure solution, Acta Crystallogr. D Biol. Crystallogr. 66 (2010) 213–221, http://dx.doi.org/10.1107/S0907444909052925. <http://scripts.iucr.org/cgi-bin/paper?dz5186> (accessed14.03.2013).

[17] P. Emsley, B. Lohkamp, W.G. Scott, K. Cowtan, Features and development of Coot, Acta Crystallogr. D Biol. Crystallogr. 66 (2010) 486–501, http://dx.doi.org/10.1107/S0907444910007493. <http://scripts.iucr.org/cgi-bin/paper?ba5144> (accessed 14.03.2013).

[18] A.T. Brunger, P.D. Adams, G.M. Clore, et al., Crystallography & NMR system: a new software suite for macromolecular structure determination, Acta Crystallogr. D Biol. Crystallogr. 54 (1998) 905–921, http://dx.doi.org/10.1107/S0907444998003254. <http://scripts.iucr.org/cgi-bin/paper?S0907444998003254> (accessed 14.03.2013).

[19] R.A. Laskowski, M.W. MacArthur, D.S. Moss, J.M. Thornton, PROCHECK: a program to check the stereochemical quality of protein structures, J. Appl. Crystallogr. 26 (1993) 283–291, http://dx.doi.org/10.1107/S0021889892009944. <http://scripts.iucr.org/cgi-bin/paper?pii=S0021889892009944&sentby=wiley> (accessed 14.03.2013).

[20] C.A. Johnston, C.Q. Doe, K.E. Prehoda, Structure of an enzyme-derived phosphoprotein recognition domain, PLoS ONE 7 (2012) e36014, http://dx.doi.org/10.1371/journal.pone.0036014. <http://www.plosone.org/article/info%3Adoi%2F10.1371%2Fjournal.pone.0036014> (accessed 1.03.2013).

[21] A.W. McGee, S.R. Dakoji, O. Olsen, et al., Structure of the SH3-guanylate kinase module from PSD-95 suggests a mechanism for regulated assembly of MAGUK scaffolding proteins, Mol. Cell 8 (2001) 1291–1301, http://dx.doi.org/10.1016/S1097-2765(01)00411-7. <http://www.sciencedirect.com/science/article/pii/S1097276501004117> (accessed 1.03.2013).

[22] G.A. Tavares, E.H. Panepucci, A.T. Brunger, Structural characterization of the intramolecular interaction between the SH3 and guanylate kinase domains of PSD-95, Mol. Cell 8 (2001) 1313–1325, http://dx.doi.org/10.1016/S1097-2765(01)00416-6. <http://www.sciencedirect.com/science/article/pii/S1097276501004166> (accessed 1.03.2013).

[23] J. Blaszczyk, Y. Li, H. Yan, X. Ji, Crystal structure of unligated guanylate kinase from yeast reveals GMP-induced conformational changes, J. Mol. Biol. 307 (2001) 247–257, http://dx.doi.org/10.1006/jmbi.2000.4427. <http://www.sciencedirect.com/science/article/pii/S0022283600944279> (accessed 1.03.2013).

[24] C.A. Johnston, D.S. Whitney, B.F. Volkman, et al., Conversion of the enzyme guanylate kinase into a mitotic-spindle orienting protein by a single mutation that inhibits GMP-induced closing, Proc. Natl. Acad. Sci. USA 108 (2011) E973–978, http://dx.doi.org/10.1073/pnas.1104365108. <http://www.pnas.org/content/108/44/E973.short> (accessed 1.03.2013).

[25] M.F. Lye, A.S. Fanning, Y. Su, et al., Insights into regulated ligand binding sites from the structure of ZO-1 Src homology 3-guanylate kinase module, J. Biol. Chem. 285 (2010) 13907–13917. <http://www.jbc.org/content/285/18/13907.short> (accessed 1.03.2013).

[26] J. Nomme, A.S. Fanning, M. Caffrey, et al., The Src homology 3 domain is required for junctional adhesion molecule binding to the third PDZ domain of the scaffolding protein ZO-1, J. Biol. Chem. 286 (2011) 43352–43360, http://dx.doi.org/10.1074/jbc.M111.304089. <http://www.jbc.org/content/286/50/43352.short> (accessed 1.03.2013).

[27] L. Pan, J. Chen, J. Yu, et al., The structure of the PDZ3-SH3-GuK tandem of ZO-1 protein suggests a supramodular organization of the membrane-associated guanylate kinase (MAGUK) family scaffold protein core, J. Biol. Chem. 286 (2011) 40069–40074, http://dx.doi.org/10.1074/jbc.C111.293084, doi: 10.1074/jbc.M109.093674. <http://www.jbc.org/content/286/46/40069.short> (accessed 1.03.2013).

[28] R.A. Newman, K.E. Prehoda, Intramolecular interactions between the Src homology 3 guanylate kinase domains of discs large regulate its function in asymmetric cell division, J. Biol. Chem. 284 (2009) 12924–12932, http://dx.doi.org/10.1074/jbc.M809304200. <http://www.jbc.org/content/284/19/12924.short> (accessed 1.03.2013).

[29] D.F. Woods, C. Hough, D. Peel, et al., Dlg protein is required for junction structure, cell polarity, and proliferation control in *Drosophila* epithelia, J. Cell Biol. 134 (1996) 1469–1482, http://dx.doi.org/10.1083/jcb.134.6.1469. <http://jcb.rupress.org/content/134/6/1469.abstract> (accessed 1.03.2013).

[30] J.L. Round, L.A. Humphries, T. Tomassian, et al., Scaffold protein Dlgh1 coordinates alternative p38 kinase activation, directing T cell receptor signals toward NFAT but not NF-κB transcription factors, Nat. Immunol. 8 (2006) 154–161, http://dx.doi.org/10.1038/ni1422. <http://www.nature.com/ni/journal/v8/n2/full/ni1422.html> (accessed 1.03.2013).

[31] I. Paarmann, O. Spangenberg, A. Lavie, M. Konrad, Formation of complexes between Ca^{2+}· calmodulin and the synapse-associated protein SAP97 requires the SH3 domain-guanylate kinase domain-connecting HOOK region, J. Biol. Chem. 277 (2002) 40832–40838, http://dx.doi.org/10.1074/jbc.M205618200. <http://www.jbc.org/content/277/43/40832.full> (accessed 1.03.2013).

[32] R.A. Lue, S.M. Marfatia, D. Branton, A.H. Chishti, Cloning and characterization of hdlg: the human homologue of the Drosophila discs large tumor suppressor binds to protein 4.1, Proc. Natl. Acad. Sci. USA 91 (1994) 9818–9822, http://dx.doi.org/10.1073/pnas.91.21.9818. <http://www.pnas.org/content/91/21/9818.abstract> (accessed 1.03.2013).